

The photo-Fries rearrangement of 9-trimethylsilyl substituted xanthenes

Michael G. Siskos^{a,*}, Antonios K. Zarkadis^{a,*}, Panagiotis S. Gritzapis^a, Ortwin Brede^{b,1},
Ralf Hermann^{b,1}, Vasilios S. Melissas^a, Gagik G. Gurzadyan^{c,2},
Anastasios S. Triantafyllou^a, Vasilios Georgakilas^a

^a Department of Chemistry, University of Ioannina, 45110 Ioannina, Greece

^b Interdisciplinary Group of Time-Resolved Spectroscopy, University of Leipzig, Permoserstrasse 15, D-04303 Leipzig, Germany

^c Technical University of Munich, Institute of Physical & Theoretical Chemistry, Lichtenbergstr 4, D-85748 Garching, Germany

Received 18 November 2005; received in revised form 31 December 2005; accepted 11 January 2006

Available online 17 February 2006

Abstract

In this paper, the absorption and fluorescence spectra of xanthene, 9-trimethylsilyl xanthene (**1**) and 9-methyl-9-trimethylsilyl xanthene (**2**) are presented and discussed with the help of CNDO/S and ab initio calculations. Introduction of the trimethylsilyl group at the 9-position of the xanthene molecule considerably shifts the short-wavelength band (246 nm) to the red and reduces the fluorescence quantum yields ($\Phi_f = 0.03$ for xanthene, 0.008 for **1** and $<10^{-4}$ for **2** in MeCN) and the fluorescence lifetimes ($\tau_f = 7.4$ ns for xanthene, 220 ps for **1** and <100 ps for **2** in MeCN), while it does not affect seriously the long-wavelength band and the singlet excited state energies ($E_S = 97.7$ kcal/mol for xanthene, 94.5 kcal/mol for **1** and 97.4 kcal/mol for **2** in MeCN). Ab initio calculations predict a 'roof-like' structure for **1** with folding angles 30° for the S_0 and 20° for the S_1 state. Laser (248, 266 and 308 nm) and lamp photolysis (254 nm) of **1** and **2** (MeCN or cyclohexane) results in [1,3]-trimethylsilyl rearrangement into the ortho-position of the xanthene moiety in the sense of a photo-Fries type reaction. The corresponding photo-Fries intermediates (exocyclic cyclohexatrienes: trimethyl-(1*H*-xanthen-1-yl)-silane, **1CHT** and trimethyl-(9-methyl-1*H*-xanthen-1-yl)-silane, **2CHT**) are formed within the 20 ns laser pulse and show absorption spectra peaking up at 410 and 403 nm, respectively. Additionally, small amounts of the corresponding 9-xanthyl radicals were detected as a result of the C–Si bond rupture. Using ps-laser flash photolysis (266 nm laser, MeCN) we observed a broad absorption spectrum peaking up at 960 nm and decaying monoexponentially with a lifetime of 130 ps, close to the measured fluorescence lifetime. We assigned therefore this transient to the singlet excited state of **1** ($S_1 \rightarrow S_n$ absorption). We assume the S_1 state as the origin of the photo-Fries rearrangement, giving via C–Si bond dissociation a singlet geminal radical pair (9-xanthyl radical + $\cdot\text{SiMe}_3$). In the next step, the radical pair undergoes predominantly in-cage recombination to the persistent photo-Fries intermediates with high quantum yields ($\Phi_{\text{1CHT}} = 0.70$ and $\Phi_{\text{2CHT}} = 0.50$), while to a lesser extent it escapes the solvent cage ($\Phi = 0.30$ for **1**) and undergoes typical free radical reactions (e.g., scavenging with O_2). The estimation of the above quantum yields was possible only after determination of the absorption coefficients (ϵ) of the photo-Fries intermediates [$\epsilon_{\text{1CHT}}(410 \text{ nm}) = 16,800 \text{ M}^{-1} \text{ cm}^{-1}$ and $\epsilon_{\text{2CHT}}(403 \text{ nm}) = 15,900 \text{ M}^{-1} \text{ cm}^{-1}$] using three independent methods; this represents the first example in the literature.

© 2006 Elsevier B.V. All rights reserved.

Keywords: Photo-Fries rearrangement; Trimethylsilyl xanthenes; Laser flash photolysis; Fluorescence; Ab initio

1. Introduction

The photochemistry of organosilicon compounds has been the subject of numerous investigations in recent years. Examples of reactions extensively studied include the photo-oxidative

cleavage of the C–Si bond of various benzylsilanes, alkylsilanes, disilanes, etc. [1–3]. We also have studied the C–Si splitting of benzylsilane radical cations produced by pulse radiolysis in *n*-BuCl, and found two decomposition channels corresponding to the equilibrium of their conformer distribution [4].

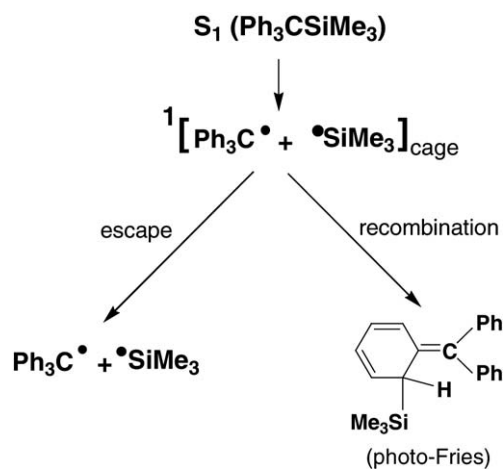
On the contrary, studies on the direct photolysis of benzylsilanes are scarcely and questions regarding the mechanism of the C–Si bond cleavage and the responsible excited states are still open being the subject of considerable debate. Kira et al. [5] and particularly Hiratsuka et al. [6] studied the photolysis of $\text{PhCH}_2\text{–SiMe}_3$ [5,6] and $\text{Ph}_2\text{CH–SiMe}_3$ [6] and suggested

* Corresponding authors. Tel.: +30 26510 98379; fax: +30 26510 98799.

E-mail addresses: azarkad@cc.uoi.gr (A.K. Zarkadis), brede@mpgag.uni-leipzig.de (O. Brede).

¹ Tel.: +49 34123 52715; fax: +49 34123 52317.

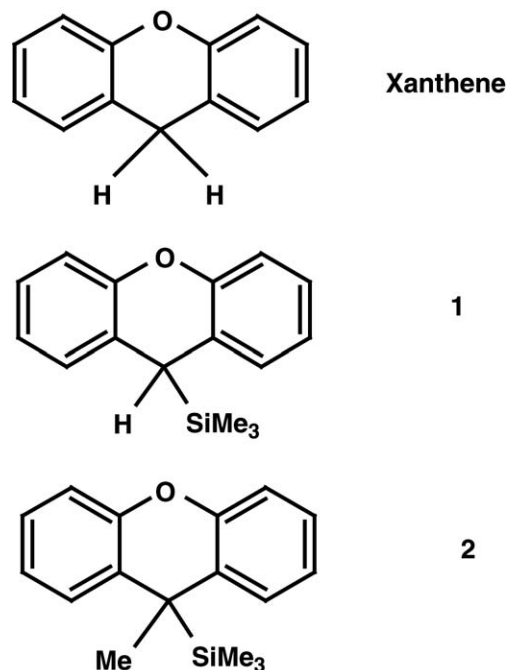
² Tel.: +49 89289 13449; fax: +49 89289 13026.



that the primary photochemical event is the formation of photo-Fries rearranged products (metathesis of the Me_3Si -group from the benzylic to the *ortho*-ring position). They found also minor amounts of the radicals PhCH_2^\bullet , $\text{Ph}_2\text{CH}^\bullet$ stemmed from the homolysis of the benzylic carbon–silicon bond. We also found recently a similar photochemical behavior by the photolysis of $\text{Ph}_3\text{C}-\text{SiMe}_3$ [7]. Using absorption ns- and fs-laser flash photolysis (LFP), electron spin resonance spectroscopy (ESR) and product analysis studies we were able to monitor all the consecutive steps towards the C–Si bond homolysis as well as the final products; namely (Scheme 1), (i) the formation of the S_1 state, which is depopulated by C–Si bond lysis, (ii) the formation of trityl radicals (within ~ 0.5 ps), which partly escaped the solvent cage (quantum yield $\Phi \approx 0.16$) and (iii) the photo-Fries cyclohexatrienyl intermediate ($\Phi \approx 0.85$) as an in-cage recombination product (within ca. 10 ps).

On the other hand, we identified only triplet state-mediated radical products ($\Phi = 0.90$) and almost no rearrangements if we introduced on the *p*-position of the silane $\text{Ph}_3\text{C}-\text{SiMe}_3$ the *p*-benzoyl or the *p*-dimethylamino group, as in *p*- $\text{PhCO}-\text{C}_6\text{H}_4-\text{C}(\text{SiMe}_3)\text{Ph}_2$ or *p*- $\text{Me}_2\text{N}-\text{C}_6\text{H}_4-\text{C}(\text{SiMe}_3)\text{Ph}_2$, respectively. Obviously, the triplet state formed in that case due to an effective intersystem crossing (ISC) gives a triplet radical pair which escapes from the solvent cage before recombination occurs. Triplet-derived radical products were also reported by Leigh and Sluggett by photolytical studies on phenyldisilanes using triplet sensitizers [3c].

In the present work, we have extended our studies on organosilicon compounds which give photo-Fries products, with two new bridged compounds, 9-(trimethylsilyl)-xanthene (**1**) and 9-(methyl)-9-(trimethylsilyl)-xanthene (**2**), see Scheme 2. We describe their photophysical properties in respect to xanthene [8], and their photochemical behavior using UV–vis, fluorescence, laser flash photolysis (LFP) in the ns- and ps-timescale, and assisted by the pulse radiolysis technique and ab initio calculations. A major contribution of the present study constitutes the quantitative description of the photoconversion which was possible only after determination of the absorption coefficients (ϵ) of the photo-Fries intermediates.



2. Experimental

2.1. Material and methods

2.1.1. Material and reagents

Acetonitrile, hexane and cyclohexane (Merck) were of spectroscopic grade. *n*-Butyl chloride has been purified by treating it with molecular sieve (A4, X13) and distillation under nitrogen. 9-(Trimethylsilyl)-9H-xanthene (**1**) [9a] and 9-(triphenylsilyl)-9H-xanthene [9b] have been previously described.

9-Methyl-9-(trimethylsilyl)-9H-xanthene (2): This compound was prepared by adding a suspension of 2.0 g (8 mmol) of compound **1** in 20 ml of abs. ether into a solution (8.8 mmol) of *n*-BuLi in 20 ml of abs. ether. After 5 h reflux, a solution of 1.3 g (9 mmol) of MeI in abs. ether was added drop wise and the mixture was refluxed overnight. After hydrolysis, extraction with ether, drying with magnesium sulfate and evaporation of the solvent, 1.4 g (67%) of compound **2** was isolated and recrystallized from ethanol, white crystals, mp 122–123 °C; ν_{max} (KBr) 3076, 3031, 2963, 2917, 2867, 1593, 1569, 1474, 1435, 1378, 1292, 1284, 1243, 1126, 1097, 1025, 941, 838 (C–Si), 778, 750 and 686 cm^{-1} ; ^1H NMR (250 MHz, CDCl_3): δ_{H} (ppm) = 6.97–7.18 (8H, m, Ar–H), 1.75 (3H, s, CH_3), –0.01 (9H, s, SiMe_3); ^{13}C NMR (68.8 MHz, CDCl_3): δ_{C} (ppm) = 151.6, 128.7, 126.2, 125.7, 122.9, 115.9 (C_{arom}), 31.2 ($\text{CMe}-\text{SiMe}_3$), 18.6 ($\text{CMe}-\text{SiMe}_3$), 1.03 (SiMe_3); MS: 268.43 (*m/e*), 268 (M^+ , 11%), 253 (4%), 195 (100%, M^+-SiMe_3), 165 (20%), 73 (37%, SiMe_3).

2.1.2. Absorption and fluorescence measurements

Absorption spectra were obtained with a Perkin-Elmer Lambda-16 spectrophotometer and fluorescence spectra measurements using a Perkin-Elmer Model LS-50B fluorescence

spectrometer at 25 °C and corrected for the response of the instrument. Fluorescence quantum yields were measured by the relative method using quinine sulfate as the standard (0.546 in 0.5 mol l⁻¹ H₂SO₄) [10a].

Fluorescence lifetime measurements were carried out using the single-photon counter FL900 (Edinburgh Instruments).

2.1.3. Steady-state UV photolyses

The photolyses were performed at 254 nm with a Heraeus TNN-15 W low pressure mercury lamp at 20 °C in quartz cuvettes. The photolysis solutions (~1 mM) were purged with argon or oxygen before irradiation.

2.1.4. ns-Laser flash photolysis

Solutions of compound **1** (A/cm ~1.0 for the 248 nm and ~0.5 for the 308 nm laser) were deoxygenated by bubbling with argon or purged with oxygen and photolysed at 20 °C in a flow system (Suprasil quartz cell) using 20 ns pulses (0.3–100 mJ) of 248 nm light (KrF*) from a Lambda Physik EMG 103MSC excimer laser or 308 nm light (XeCl*) from Lambda Physik EMG150E laser. The solutions (A/cm ~0.8) of compound **2** were photolysed by the fourth harmonics (266 nm) of a Quanta-Ray GCR-11 Nd:YAG laser (Spectra Physics, pulse duration <3 ns) with energies of 0.5–10 mJ. The optical detection system consisted of a pulsed xenon lamp (XBO 450, Osram), a monochromator (Spectra Pro 275, Acton Research Corporation), an R955 photomultiplier tube (Hamamatsu Photonics) or a fast Si-photodiode with 1 GHz amplification, and a 500 MHz digitizing oscilloscope (DSA 602 A, Tektronix).

2.1.5. Quantum yields

The quantum yields for the formation of the 9-xanthyl radicals and photo-Fries products **1CHT** and **2CHT** produced by the photolysis of **1** and **2**, respectively (MeCN), were determined by measuring the initial absorbance at λ_{\max} under N₂ and under oxygen. As reference (actinometer) was used the triplet state of benzophenone ($\Phi_{\text{triplet}} = 1$) [11] at 525 nm produced under identical conditions (the same optical density at 266 nm, OD = 0.3/cm). The measurements were carried out with varying laser intensity (0–15 mJ/pulse) and by plotting the absorbance versus the laser intensity [10b]. The slope under oxygen corresponds to the photo-Fries product, while the difference of the slopes under N₂ and under oxygen corresponds to the 9-xanthyl radicals. We used values of $\epsilon(\text{triplet benzophenone}) = 6500 \text{ M}^{-1} \text{ cm}^{-1}$ at 525 nm [10c], $\epsilon(9\text{-xanthyl radical}) = 22,000 \text{ M}^{-1} \text{ cm}^{-1}$ at 348 nm [12b] and $\epsilon(\mathbf{1CHT}) = 16,800 \text{ M}^{-1} \text{ cm}^{-1}$ at 410 nm and $\epsilon(\mathbf{2CHT}) = 15,900 \text{ M}^{-1} \text{ cm}^{-1}$ at 403 nm (see Section 3.3).

2.1.6. ps-Laser flash photolysis

The picosecond spectrometer is described previously [13,14], and it is based on a mode-locked Nd:YAG laser (Continuum PY61C-10), $\lambda_{\text{fundamental}} = 1.064 \mu\text{m}$, pulse width 30 ps, pulse repetition rate 10 Hz, pulse energy per shot 40 mJ. Light at $\lambda = 266 \text{ nm}$ (2–3 mJ), obtained by fourth harmonics in KDP non-linear crystals was used for excitation. A white light continuum ($\lambda = 420\text{--}1050 \text{ nm}$) generated upon propagation of the 1.064 μm

fundamental beam through a 13 cm quartz flow cell filled with D₂O was used as a probe beam. The time delay between the pump and probe beams could be varied in the range 0–10 ns by a step-motor driven (7 fs step) and computer-controlled delay line. The angle between the excitation and white light probing beams was 90°. A quartz flow cell system was used. A PC with the help of Lab VIEW (National Instruments) software carried out automated performance of the set-up, e.g., manipulation of the delay line and the shutter, as well as the data processing.

2.1.7. ns-Pulse radiolysis

The liquid samples purged with nitrogen or oxygen were irradiated with high energy electron pulses (1 MeV, 12 ns duration) generated by a pulse transformer electron accelerator ELIT (Institute of Nuclear Physics, Novosibirsk, Russia). The dose delivered per pulse was measured using the absorbance of the solvated electron in slightly alkaline aqueous solution, and was usually around 100 Gy. Detection of the transient species was carried out using an optical absorption technique, consisting of a pulsed xenon lamp (XBO 450, Osram), a Spectra Pro 500 monochromator (Acton Research Corporation), an R955 photomultiplier (Hamamatsu Photonics) and a 1 GHz digitizing oscilloscope (TDS 640, Tektronix).

2.2. Theory and calculations

Ab initio and semi-empirical (PM3, AM1) calculations were performed using the GAUSSIAN 98 suite of programs [15a]. A complete optimization for the neutral form of the molecule was initially carried out at the HF/cc-pVTZ level of theory [15b], followed by vibrational analysis for a complete verification that the obtained stationary point corresponds to a true minimum. A singlet excited state calculation was performed with the cc-pVTZ basis set and the configuration interaction approach, which models excited states as combinations of single contributions out of the Hartree–Fock ground state, namely CIS [15c,d]. The CIS description of the excited states is considered to be a zeroth-order one, providing reasonable integral storage and transformation requirements in case of polyatomic molecules [15e]. The CNDO/S method [15f] was used to calculate the absorption maxima and oscillator strengths (*f*) after geometry optimization using PM3.

3. Results and discussion

3.1. Absorption and fluorescence spectra

Absorption data of xanthene and its silicon derivatives **1** and **2** in hexane (or cyclohexane), MeCN and MeOH (a non-polar, a polar and a hydrogen bonding solvent) are listed in Table 1. They all show a broad absorption band at 280–290 nm (see, for example, Figs. 1 and 2). Xanthene (Fig. 2) itself shows an additional band at 245 nm which is absent in **1** and **2**. All the absorption bands do not show any significant dependence on solvent polarity or protic ability, and the fluorescence excitation spectra are similar to the absorption spectra.

Table 1
Absorption and emission wavelength maxima, fluorescence lifetimes (τ_f), fluorescence quantum yields (Φ_f) and singlet excited state energies (E_S)

Solvent	Absorption		Emission				
	λ_{\max} (nm)	ϵ ($10^3 \text{ M}^{-1} \text{ cm}^{-1}$)	λ_{\max} (nm)	τ_f (ns)	Φ_f	$\lambda_{0,0}$ (nm)	E_S (kcal/mol) ^c
Xanthene							
<i>n</i> -Hexane	246 (246) ^a , 283 (281) ^a	8.2, 2.4	295, 305		0.03 ^b	92.8	97.7
MeCN	245, 282	7.8, 2.6	296, 306	7.4	0.02	292.6	97.7
EtOH	244, 285	3.9, 3.4					
1							
<i>n</i> -Hexane	280 (279) ^a	3.3	316	0.21	0.0007	299.6	95.4
MeCN	280	4.5	330	0.22	0.0008	302.5	94.5
MeOH	280	3.4	331		0.0009	300.6	95.1
2							
Cyclohexane	283 (281) ^a	4.2					
MeCN	283	5.6	~330	<0.1	<10 ⁻⁴	293.6	97.4
MeOH	283	3.3					

^a In parentheses, the CNDO/S calculated values.

^b A value of 0.05 was reported in ref. [8b].

^c A value of $E_S = 97.5$ kcal/mol in EtOH at 77 K was reported for xanthene in ref. [8a] and a value of $E_S = 99.3$ kcal/mol from jet-cooled xanthene in ref. [9].

The absorption and the fluorescence spectra of xanthene (Fig. 2) exhibit a well-defined vibronic structure in hexane and to a lesser degree in MeCN. A good mirror-image relationship is observed between the absorption and fluorescence spectra with little Stokes-shift indicating similar geometries for the ground and the first excited state. Additionally, the solvent independence of both spectra (absorption and emission) shows that the dipole moment does not change appreciably on excitation. Based on the fluorescence excitation spectra of jet-cooled xanthene,

Chakraborty and Lim [16] concluded that the molecule is planar in the S_1 excited state and slightly non-planar in the S_0 , while a variety of calculations predict a planar ground state S_0 [17]. Considering now the absorption spectra of **1** and **2**, is not surprising the absence of the absorption band at ~ 245 nm; if the hydrogen at the 9-position of xanthene is replaced by a SiMe_3 group, the band at ca. 283 nm remains unaffected while a considerable red shift of the second xanthene band (245 nm) forces them to overlap. This is also observed in the absorption spectra of the series PhCH_3 , $\text{PhCH}_2\text{-SiMe}_3$, $\text{Ph}_2\text{CH-SiMe}_3$ [6a] and

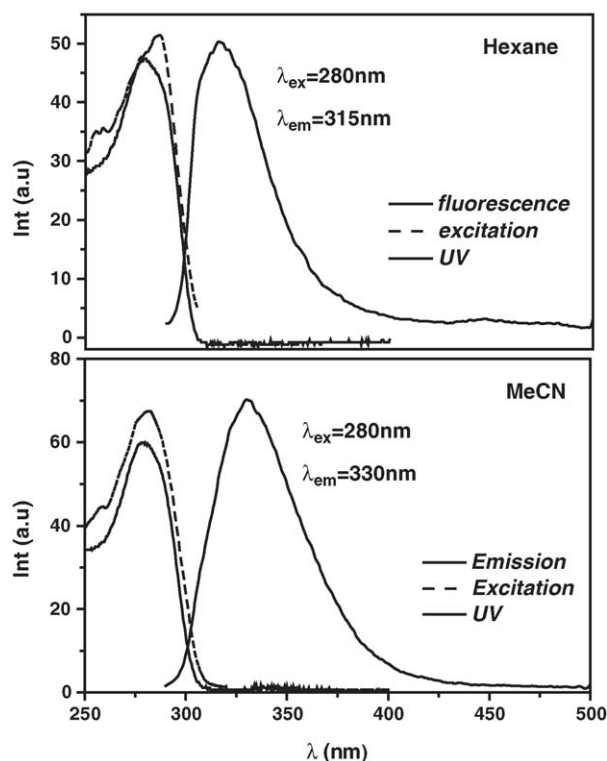


Fig. 1. Absorption, fluorescence (solid lines) and fluorescence excitation (broken line) spectra of 9-trimethylsilyl xanthene **1** in *n*-hexane and MeCN at 298 K.

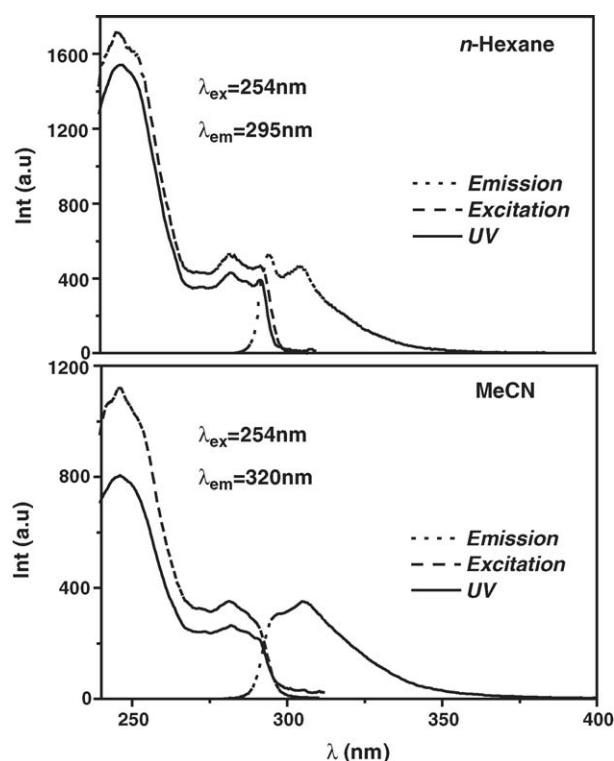


Fig. 2. Absorption (solid line), fluorescence (dotted line) and fluorescence excitation (broken line) spectra of xanthene in *n*-hexane and MeCN at 298 K.

PhCH(Me)–SiMe₃, PhC(Me)₂–SiMe₃, Ph₂CH–SiMe₃ [7b], and is attributed to the interaction of the σ -molecular orbital of the C–Si bond with the π -molecular orbital of the aromatic system through the hyperconjugative effect (β -silicon effect) [18a–f] and a probable contribution by the inductive (+I) effect of the CH₂SiMe₃ group (Hammett constants: $\sigma_m = -0.16$, $\sigma_p = -0.21$) [18g]. It is found [18a–e] that this raises the energy level of the π -orbital, while simultaneously affects little the π^* -unoccupied orbital of the aromatic system. The overlapping of the two bands makes the absorption spectrum broader and increases the absorption intensity of the long-wave band. The above interpretation is supported by CNDO/S calculations (Table 1), which predict a red shift from 246 to 258 nm for silane **1**. Compared to Ph₂CH–SiMe₃, silyl xanthene **1** enables a more effective hyperconjugative interaction of the C–Si bond with the π system due to the methylene- and oxygen-bridges (rigid molecular backbone) and therefore causes a larger bathochromic shift as was also experimentally observed. Ab initio calculations for **1** predict an almost perpendicular arrangement (84.5°) of the C–Si bond in respect to the aromatic system, ideal for hyperconjugative interaction.

The fluorescence spectra of both silicon derivatives **1** and **2** show a considerable dependence on the solvent polarity and the emission maximum is shifted from 316 nm in hexane to 330 nm in MeCN (to 331 nm in MeOH) increasing the Stokes-shift. This is in contrast to the solvent independence of their absorption spectra and to the insensitivity of both the absorption and emission spectra in the case of xanthene (Table 1). This solvent effect on fluorescence emission is associated with the dipolar rearrangement of the solvent shell in the excited state of the molecule and is typical for molecules that undergo a change in dipole moment upon electronic excitation.

Ab initio calculations have been performed for the ground (S_0) and singlet excited state (S_1) of compound **1**. They predict for S_0 a ‘butterfly’ conformation shown in Fig. 3 with a fold angle of 30°. The central ring acquires a boat conformation. Analogous folding angles of the range 14–30° were found in crystallographic studies of 9-isopropyl-xanthene (21.9°) [19], methyl-9-xanthyl ketone (30.1°) [20] or xanthene-9-carboxylic acid (14.2°) [21]. The singlet excited state (S_1) was found to possess a similar structure with reduced folding angle (~20°). However, on excitation ($S_0 \rightarrow S_1$) the calculation predicts (i)

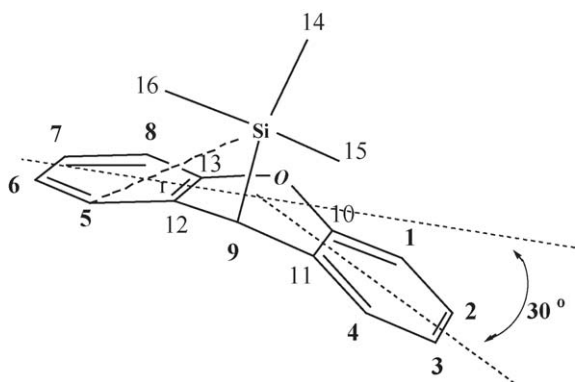


Fig. 3. Ab initio optimized structure of compound **1** in the S_0 state.

10° planarization, (ii) increased charge delocalization from oxygen to the aromatic ring (charge at oxygen -0.32 in S_0 and -0.27 in S_1), (iii) lengthening of the C9–Si bond (1.936 Å in S_0 and 1.987 Å in S_1) and (iv) slight increase of the dipole moment ($\mu_{S_0} = 1.16$ D to $\mu_{S_1} = 1.32$ D). In contrast to the ab initio results, the semi-empirical PM3 or AM1 calculations predict for the S_0 state of **1** a planar geometry and a folded one for **2**. The ab initio results are in reasonable agreement with the photophysical data presented above; the slight planarization predicted for the S_1 state and consequently the increasing of the dipole moment explains the small Stokes-shift observed and the solvent dependence of the fluorescence emission spectra.

A final comment deserves the observed drastic reduction of the fluorescence quantum yields ($\Phi_f = 0.03$ in xanthene, 0.0008 in **1** and $<10^{-4}$ in **2**) and fluorescence lifetimes ($\tau_f = 7.4$ ns in xanthene, 0.22 ± 0.06 ns in **1** and <0.1 ns in **2**) observed upon the introduction of the SiMe₃ group into the xanthene moiety (Table 1). This is indicative of an increased photoreactivity of **1** and **2** and this constitutes the main subject of the present work.

3.2. ns-Laser flash photolysis studies

3.2.1. Photolysis of **1** in MeCN with 248 or 308 nm laser

The spectrum shown in Fig. 4a was obtained by photolysis of a deoxygenated (argon) MeCN solution of **1** (0.62 mM) with 248 nm laser light (20 ns pulses). It displays a broad peak with maximum at about 410 nm, which remains unchanged from the ns to ms time regime.

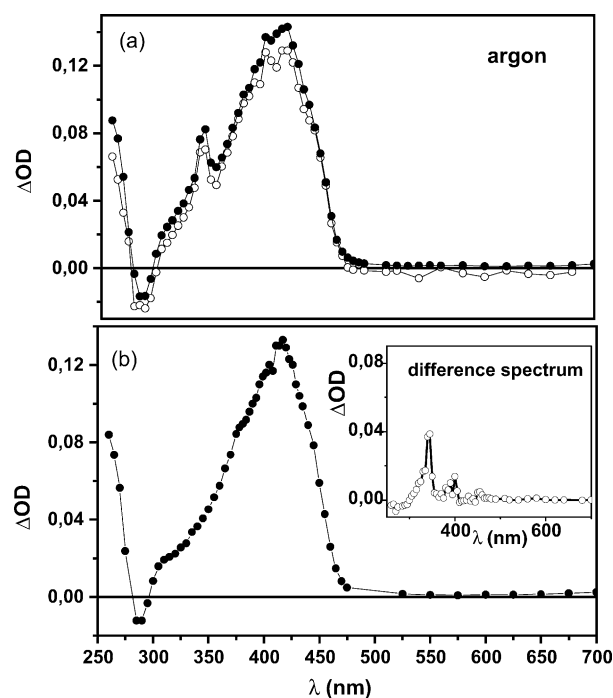


Fig. 4. (a) Absorption spectrum obtained on 248 nm LFP of 0.62 mM of **1** in MeCN under argon recorded at 30 ns (open circles) and 15.5 μ s (solid circles) after the pulse and (b) under oxygen atmosphere 20.5 μ s after the pulse. *Inset*: Difference spectrum obtained between the argon and oxygen spectra at 20.5 μ s after the pulse.

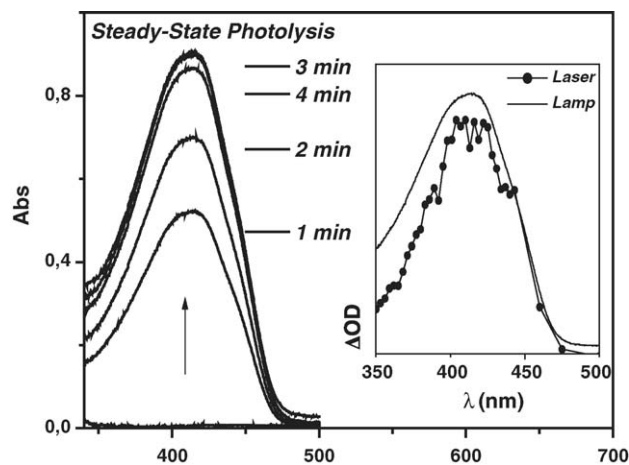
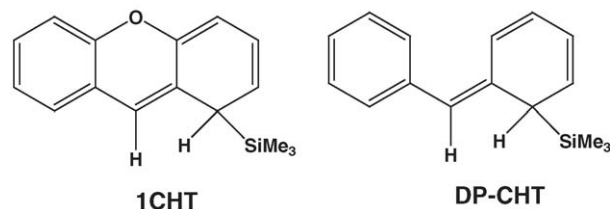


Fig. 5. Absorption spectrum obtained by steady-state lamp irradiation (254 nm low pressure Hg-lamp) of **1** in cyclohexane under oxygen (1.0 mM). Inset: Comparison of the transients produced via 248 nm LFP and steady-state photolysis (lamp).

Additionally, a very small narrow absorption peak was detected as a shoulder at 345 nm. At ca. 280 nm, the bleaching of the parent compound was clearly visible as a negative peak and remains nearly constant with the time; this is an indication that the parent compound is not regenerated, but it undergoes an irreversible transformation to the stable transient species absorbing at 410 nm.

When oxygen was admitted to the solution an almost identical spectrum was produced, insensitive to oxygen, with the only difference the absence of the little sharp peak at 345 nm. The differential absorption spectrum produced by subtracting the two transient spectra (Fig. 4a and b) is depicted as inset in Fig. 4b. This absorption has a maximum at ~ 345 nm and is very similar to that reported for the 9-xanthyl radical (**1 \bullet**). From the difference in the absorbance at 345 nm (N_2 -spectrum versus O_2 -spectrum, Fig. 4, see also Section 2) and the known absorption coefficient ($\epsilon = 22,000 \text{ M}^{-1} \text{ cm}^{-1}$ at 348 nm) [12b] of **1 \bullet** , we found the quantum yield $\Phi_1^\bullet = 0.3$ for the radical formation. The stability of the insensitive to O_2 transient, prompted us to check if the same species occurs by steady-state lamp irradiation. In Fig. 5, the stationary UV spectrum is shown which increases with the irradiation time (see Section 2). On prolonged irradiation a slight decrease of the signal was observed, while keeping the irradiated solution in the dark overnight the absorption was completely disappeared. The same absorption spectra and the same behavior were observed in cyclohexane, MeCN and MeOH. In the inset of Fig. 5, the spectra obtained with LFP and lamp irradiation (oxygen atmosphere) are presented for comparative reasons. We attributed this very stable transient to the cyclohexatriene intermediate **1CHT** formed via a [1,3]-trimethylsilyl rearrangement in the sense of a photo-Fries type reaction (Scheme 3). This is a typical rearrangement we also found by the photolysis of $\text{Ph}_3\text{C-SiMe}_3$ (see Scheme 1) [7a]; Hiratsuka et al. [6a] found a similar intermediate (**DP-CHT**) photolysing the diphenylmethyl derivative $\text{Ph}_2\text{CH-SiMe}_3$, Leigh and Sluggett reported in a series of papers



Scheme 3.

analogous rearrangements occurred by the photolysis of benzyl disilanes [3].

Unfortunately, we could not isolate the product; irradiation of **1**, however, direct in an NMR-tube (CD_3CN) gave ^1H NMR signals attributable to cyclohexadienyl protons of **1CHT**, while in CDCl_3 , Me_3SiCl was identified (see ^1H NMR data in Supplementary data). In the presence of traces of HCl the olefinic signals and the UV absorption band at 410 nm were removed, following the well-known acid-catalyzed re-aromatization of such systems [22]. Prolonged irradiation in the presence of oxygen gave xanthone as an oxidation product of **1CHT** or xanthyl radicals (see ^1H NMR and UV data in Supplementary data, Fig. A).

Obviously, the formation of photoproduct **1CHT** hinders an appreciable photoconversion acting itself as an inner-filter. Completely identical transient species were produced also by irradiation with 308 nm laser light (see Fig. B in Supplementary data).

Similarly behaves also the triphenylsilyl derivative 9-(Ph_3Si)-xanthene giving the corresponding photo-Fries intermediate absorbing at ca. 415 nm and the radicals 9-xanthyl and $\text{Ph}_3\text{Si}^\bullet$ (absorbing at $\lambda_{\text{max}} = 320$ nm) [12f], see Fig. C in Supplementary data.

3.2.2. Picosecond-LFP of **1** in MeCN (266 nm)

Since the intermediate **1CHT** was formed faster than the time-resolution of our nanosecond LFP apparatus (20 ns) and in order to get more insight regarding the state involved in the rearrangement, a ps-LFP experiment was performed in MeCN solution (Fig. 6a). The absorption spectrum of the transient obtained 80 ps after the laser pulse was characterized by a very broad band peaking-up at about 960 nm with a shoulder at ~ 635 nm. The 960 nm transient species decay monoexponentially with a lifetime of 130 ± 20 ps (see inset in Fig. 6a), a time comparable within the accuracy of the method with the fluorescence lifetime of 220 ± 60 ps measured by single-photon counting (Table 1). Consequently, we assign this band to the $S_1 \rightarrow S_n$ transition of **1**. The photo-Fries intermediate **1CHT** with absorption maximum at 410 nm which was detected with ns-LFP was not possible to observe because of instrument limitations monitoring only the wavelength region ≥ 450 nm.

The second band at 635 nm is long-lived and persists in the 10 ns time regime, which is the upper limit of the instrument detection (Fig. 6b). We attribute this band either to radical cation (**1 \bullet^+**) of compound **1**, in agreement with the pulse radiolytic generation of **1 \bullet^+** , see spectrum in Fig. 7 below, or alternatively to xanthone triplet state which absorbs also in that region [24b].

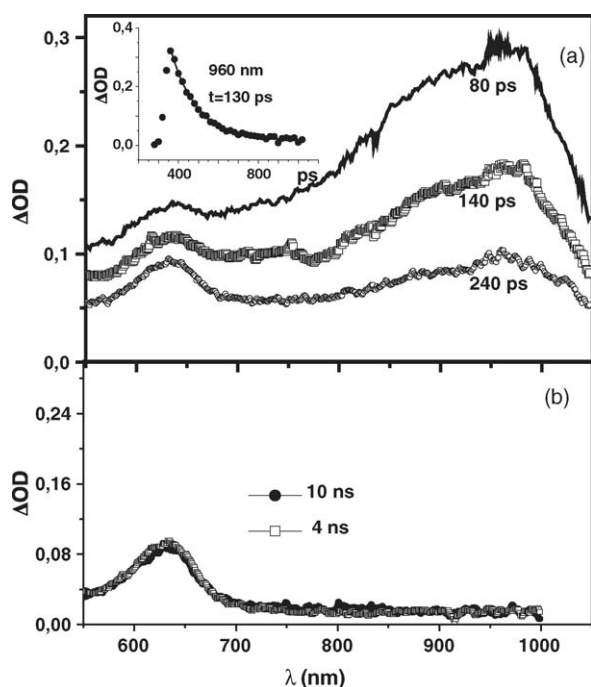


Fig. 6. (a) ps-LFP transient absorption spectra recorded at 80, 140 and 240 ps after the 266 nm excitation pulse of a solution of **1** in MeCN. Inset: The decay kinetics monitored at 960 nm and (b) the transient absorption spectrum remains unchanged at 4 and 10 ns after the pulse.

Radical cation $\mathbf{1}^{\bullet+}$ could be formed by consecutive biphotonic excitation via S_1 state (singlet–singlet two-quantum absorption). The two-quantum excitation through the T_1 state is unlikely because of the slow ISC rate constant of the benzene chromophore (ca. 0.2 μ s) [11]. Monophotonic (one-quantum) ionization process is ruled out by comparing the ionization potential of xanthone (IP = 7.65 eV [23] or 7.95 eV [24a]), with the photon energy of the excitation pulse ($\lambda = 266$ nm and $E = 4.66$ eV). Moreover, the band at 635 nm was absent during the nanosecond LFP measurements with excitation at 248 or 308 nm (see Fig. 3) because the intensity of exciting radiation using ns-LFP is much lower than the intensity of the ps-LFP (compare

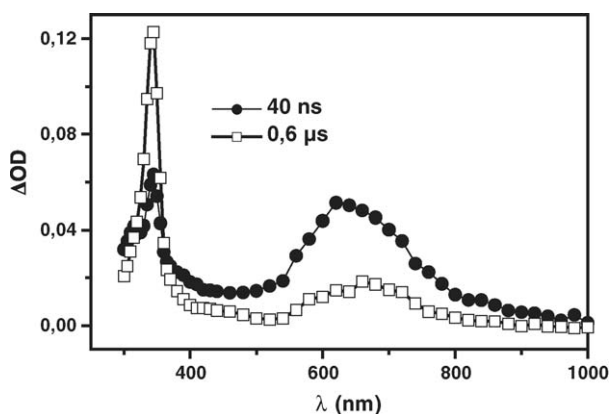


Fig. 7. Transient absorption spectra obtained via pulse radiolysis of a N_2 -purged solution of **1** (2 mM in *n*-BuCl), at 40 ns (●) and 0.6 μ s (□) after the electron pulse.

$I_{ns} = 10$ MW cm^{-2} with $I_{ps} = 500$ MW cm^{-2}). The absorption of a second photon is possible in the case of the ps-experiment because of the long singlet state lifetime (130 ps) relative to the pulse duration (~ 30 ps). In the ns-LFP experiment within the 20 ns laser pulse this possibility should be completely absent.

The radical cation $\mathbf{1}^{\bullet+}$ exhibits, however, a much broader spectrum (Fig. 7) than the absorption at 635 nm and this forces one to discuss the T_1 state of xanthone as an alternative candidate. We identified xanthone in prolonged steady-state irradiations as an oxidation product derived in the presence of atmospheric oxygen from either **1**CHT or 9-xanthyl radical or both (see 1H NMR and UV data in Supplementary data, Fig. C). The well-known [24b] spectrum of the T_1 of xanthone gives a very similar spectrum peaking-up at 630–635 nm in MeCN. Obviously, the many pulses needed in the ps-spectroscopy converts **1** partly to xanthone in the presence of oxygen.

A final point which needs further clarification is the occurrence of the 9-xanthyl radical ($\mathbf{1}^\bullet$) detected in the ns-LFP experiment in MeCN. Two ways are possible; one is the formation through the cleavage of the C–Si bond of the radical cation $\mathbf{1}^{\bullet+}$ and the other is the direct formation from the excited singlet state.

To check the first assumption, we produced the radical cation $\mathbf{1}^{\bullet+}$ independently using the pulse radiolysis technique. With this technique we obtained the transient absorption spectrum displayed in Fig. 7 (2 mM solution of **1** in *n*-BuCl, see Section 2). It consists of a broad absorption band whose decay at 640 nm is accompanied by the build-up of the absorption at 345 nm. The first band at 640 nm is attributed to $\mathbf{1}^{\bullet+}$ in analogy to spectra of many benzylsilane radical cations recently studied by us using the same technique [4a,b]. The second maximum at 345 nm we assign to radical $\mathbf{1}^\bullet$, which is formed by the C–Si bond cleavage of $\mathbf{1}^{\bullet+}$ and whose absorption spectrum is well-known in the literature [12a–e].

The radical cation $\mathbf{1}^{\bullet+}$ is a long-living species and its absence in the ns-LFP transient absorption spectrum (Fig. 4) indicates that it is not the precursor of the 9-xanthyl radical ($\mathbf{1}^\bullet$) detected by the photolysis of **1** (Fig. 4a). The radical $\mathbf{1}^\bullet$ should be therefore the product of the direct C–Si homolytic bond cleavage occurring in the S_1 surface, as we have shown recently to occur for $Ph_3C-SiMe_3$ (Scheme 1) [7a].

3.2.3. ns-Laser flash photolysis of **2** in MeCN and cyclohexane with 266 nm laser

Fig. 8a and b shows the ns-LFP spectra obtained by 266 nm photolysis of silane **2** in cyclohexane. The same spectrum was obtained also in MeCN (see Fig. D in Supplementary data). As in the case of compound **1**, a stable absorption band was detected with maximum at 403 nm and is attributed (in analogy to **1**) to the methyl cyclohexatriene intermediate **2**CHT (Scheme 4).

The stable signal was recorded immediately after the pulse and is produced monophotonically (Fig. 8a, inset). An additional narrow signal at ~ 345 nm was detected under nitrogen atmosphere, which disappears by purging oxygen into the solution; it is attributed similarly to the 9-methyl-xanthyl radical ($\mathbf{2}^\bullet$).

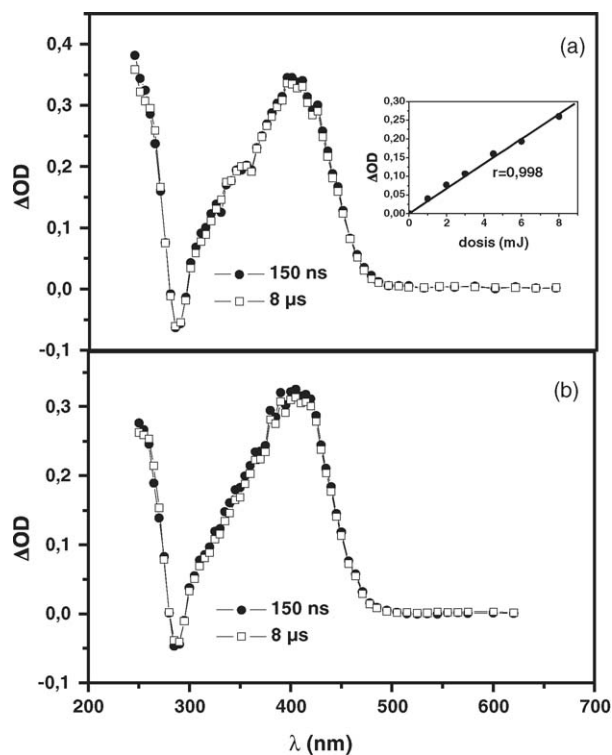
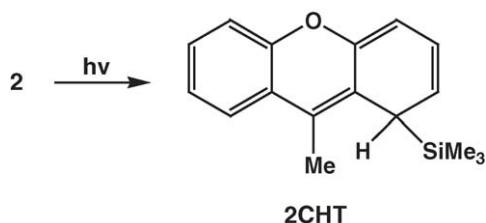


Fig. 8. Absorption spectrum obtained by photolysis of **2** (0.25 mM in cyclohexane) with 266 nm laser (a) under nitrogen. *Inset*: Spectrum intensity dependence on laser power and (b) under oxygen atmosphere.

3.3. Determination of absorption coefficients (ϵ) and formation quantum yields (Φ) of **1CHT** and **2CHT**

A major drawback of the photo-Fries reaction in general and of the present study as well, is the inability to obtain a quantitative description of the photoconversion. This is due to the lack of the absorption coefficients (ϵ) of the photo-Fries intermediates (in the present study of **1CHT** and **2CHT**) which prevents the determination of the corresponding quantum yields ($\Phi_{1\text{CHT}}$ and $\Phi_{2\text{CHT}}$). We undertook therefore several ways to determine these important ϵ values. A first estimation was possible using the oscillator strengths (f) calculated with CNDO/S ($f=0.626$ for **1CHT** and 0.611 for **2CHT**) and a useful correlation we recently found between literature ϵ values of structurally similar cyclohexatrienes and corresponding f values calculated with the same method ($\epsilon=25,748 \times f$) [7a]. We found thus $\epsilon_{1\text{CHT}}=16,100 \text{ M}^{-1} \text{ cm}^{-1}$ at 410 nm and $\epsilon_{2\text{CHT}}=15,750 \text{ M}^{-1} \text{ cm}^{-1}$ at 403 nm.



Scheme 4.

A second gross-estimation was possible using the depletion of the parent compound **1** (negative signals at 288 nm in Fig. 4) and assuming 100% total photoconversion to radical $\mathbf{1}^{\bullet} + \mathbf{1CHT}$. We found thus $\epsilon_{1\text{CHT}}=17,000 \pm 500 \text{ M}^{-1} \text{ cm}^{-1}$ and similarly $\epsilon_{2\text{CHT}}=16,000 \pm 1000 \text{ M}^{-1} \text{ cm}^{-1}$. The 100% total photoconversion is a reasonable assumption based on the very low fluorescence quantum yields and short lifetimes (see Table 1) which indicate a very fast decay of the S_1 state presumably to **1CHT** (and **2CHT**). In fact, a very fast conversion (in the sub-picosecond time scale) was measured in the case of the photo-Fries conversion of $\text{Ph}_3\text{C-SiMe}_3$ [7a].

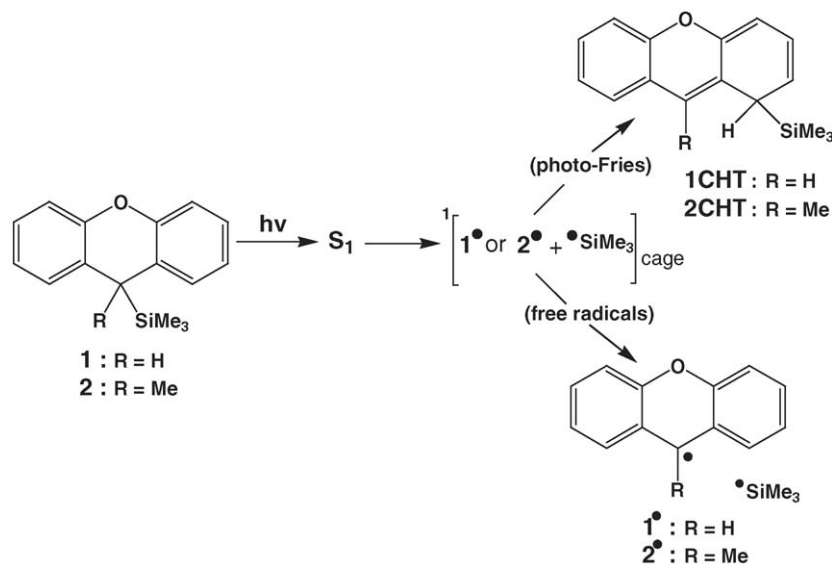
In addition, we performed colorimetric determination of the ϵ values of the photo-Fries intermediates using the stable violet coloured free radical DPPH as an analytical reagent. The method was used before by Pryor et al. [25] for the prototype 5-methylidene-1,3-cyclohexadiene. This third method gave values $\epsilon_{1\text{CHT}}=17,400 \text{ M}^{-1} \text{ cm}^{-1}$ and $\epsilon_{2\text{CHT}}=16,000 \text{ M}^{-1} \text{ cm}^{-1}$ in reasonable agreement with the other two (see details in Supplementary data, Fig. E).

Based on these values (average: $\epsilon_{1\text{CHT}}=16,800 \text{ M}^{-1} \text{ cm}^{-1}$ at 410 nm and $\epsilon_{2\text{CHT}}=15,900 \text{ M}^{-1} \text{ cm}^{-1}$ at 403 nm), we could estimate the quantum yields of formation: $\Phi_{1\text{CHT}}=0.70$ and $\Phi_{2\text{CHT}}=0.50$. This is in line with the calculated quantum yield for the radical formation ($\Phi_{\mathbf{1}^{\bullet}}=0.30$, see Section 3.2.1), indicating $\Phi_{1\text{CHT}} + \Phi_{\mathbf{1}^{\bullet}} \approx 1$, a fact which justifies the assumptions we made above. Whether the same holds also for xanthene **2** remains unresolved because $\epsilon_{\mathbf{2}^{\bullet}}$ is unknown; we believe, however, that $\Phi_{2\text{CHT}} + \Phi_{\mathbf{2}^{\bullet}} \approx 1$ in analogy to compound **1** and considering the very low fluorescence quantum yield and fluorescence lifetime (Table 1).

4. Concluding remarks

In summary, it has been shown that introduction of the trimethylsilyl group at the 9-position of the xanthene molecule (compound **1**) shifts considerably the short-wavelength band to the red and reduces the fluorescence quantum yield ($\Phi_{\text{fl}} < 0.001$) and the fluorescence lifetime ($\tau_{\text{fl}} \approx 220 \text{ ps}$) drastically. The effects are more pronounced by further substitution of the second hydrogen at the same position by a methyl group (compound **2**), see Table 1. As far as the geometry is concerned, ab initio calculations predict a 'roof-like' structure for **1** with folding angles between the phenyl rings 30° for the S_0 and 20° for the S_1 . The red shift is the result of an effective hyperconjugative interaction of the C–Si bond with the rigid molecular π -system (ab initio calculations for **1** predicts an almost ideal alignment of the C–Si bond in respect to the aromatic system, 84.5°).

Laser photolysis of **1** and **2** (248, 266 and 308 nm) in acetonitrile or cyclohexane solution results in the corresponding cyclohexatriene derivatives **1CHT** and **2CHT** and xanthyl ($\mathbf{1}^{\bullet}$) and 9-Me-xanthyl ($\mathbf{2}^{\bullet}$) radicals, respectively. A quantitative evaluation of the photoconversion was possible after the determination of the absorption coefficients (ϵ) of the photo-Fries intermediates. We determined the ϵ values using three independent methods, and found $\epsilon_{1\text{CHT}} \approx 16,800 \text{ M}^{-1} \text{ cm}^{-1}$ at 410 nm and $\epsilon_{2\text{CHT}} \approx 15,900 \text{ M}^{-1} \text{ cm}^{-1}$ at 403 nm which enabled us to determine the corresponding quantum yields $\Phi_{1\text{CHT}}=0.70$



Scheme 5.

and $\Phi_{2\text{CHT}}=0.50$ (see Section 3.3). This direct determination represents, to the best of our knowledge, the first example in the photo-Fries reaction in general. The results indicate that $\Phi_{1\text{CHT}} + \Phi_{1^{\bullet}} \approx 1$ ($\Phi_{1^{\bullet}}=0.30$, see Section 3.2.1), a fact which justifies the assumptions we made above. High photo-Fries quantum yields we also found by the photolysis of compound $\text{Ph}_3\text{C}-\text{SiMe}_3$ ($\Phi=0.85$) [7a]; high values have been also reported in the literature for the photolysis of $\text{PhSiMe}_2-\text{SiMe}_3$ ($\Phi=0.86$) [1g] as well as for the photolysis of the prototypical phenyl acetate ($\Phi=0.51$) [26].

In addition, using ps-LFP (266 nm laser, pulse duration ~ 30 ps), a short-lived transient has been recorded with maximum at 960 nm and lifetime 130 ps. We assigned it tentatively to the S_1 state on the basis of the measured fluorescence lifetime.

The results are summarized in Scheme 5 and are in line with the widely accepted mechanism of the photo-Fries reaction [27]; it states that after photoexcitation, the originally prepared S_1 state depopulates by splitting of the relevant bond (in our case the C–Si bond) and produces primarily a geminal singlet radical pair. Latter either escapes the solvent cage giving free diffusing radicals or undergoes in-cage recombination to give either the parent molecule, or photo-Fries rearranged intermediates. Only very recently using femtosecond spectroscopy was found [26] that the homolytic C–O cleavage caused by the photolysis of the prototypical phenyl acetate ($\text{PhO}-\text{COMe}$) occurs within 2 ps and the geminate recombination of the singlet radical pair to the photo-Fries intermediate cyclohexadienone needs another 13 ps. Supported by our findings for $\text{Ph}_3\text{C}-\text{SiMe}_3$ (Scheme 1), we assume a similar mechanism in the present case, although we have not been able to show unambiguously the direct involvement of the S_1 state in the generation of **1CHT** and **2CHT** (Scheme 5); we assume thus the geminal radical pair (1^{\bullet} or $2^{\bullet} + \bullet\text{SiMe}_3$) is formed by a fast C–Si bond dissociation facilitated through the high energy content of the S_1 state (95–97 kcal/mol, Table 1) and the ca. 30 kcal/mol lower C–Si bond strength (67.5 kcal/mol) [28]. The singlet geminal

radical pair arising from the originally prepared S_1 state, undergoes predominantly in-cage fast recombination to the persistent photo-Fries products **1CHT** ($\Phi=0.70$) and **2CHT** ($\Phi=0.50$) or gives to a lesser extent xanthenyl radicals (1^{\bullet} and 2^{\bullet}). The radicals escape the solvent cage and undergo typical free radical reactions as we have shown by scavenging them with oxygen (see Figs. 4b and 8b, respectively, as well as Figs. B(b), C(b) and D(b) in Supplementary data).

Acknowledgments

We thank Prof. Steen Steenken, Max-Planck-Institut für Strahlenchemie, Mülheim, Germany, for enabling us to obtain preliminary ns- and ps-LFP data and Dr. G. Pistolis, NRC Democritos (Athens) for measuring the fluorescence lifetimes. We thank the Deutscher Akademischer Austauschdienst (DAAD) and the Idryma Kratikon Ypotrofon (IKY) for financial support through the program IKYDA. A.K.Z. and M.G.S. thank DAAD for a fellowship (1998) and NMR-Center of the University of Ioannina.

Appendix A. Supplementary data

Supplementary data associated with this article can be found, in the online version, at doi:10.1016/j.jphotochem.2006.01.006.

References

- [1] (a) M.A. Brook, *Silicon in Organic, Organometallic, and Polymer Chemistry*, Wiley, NY, 2000;
- (b) A.G. Brook, in: Z. Rappoport, Y. Apeloig (Eds.), *The Chemistry of Organic Silicon Compounds*, vol. 2, Wiley, NY, 1998, p. 1233;
- (c) M.G. Steinmetz, *Chem. Rev.* 95 (1995) 1527;
- (d) E. Baciocchi, M. Bietti, O. Lanzaluna, *Acc. Chem. Res.* 33 (2000) 243–251;
- (e) K.P. Dockery, J.P. Dinnocenzo, S. Farid, J.L. Goodman, I.R. Gould, W.P. Todd, *J. Am. Chem. Soc.* 119 (1997) 1876–1883;

- (f) H. Shizuka, H. Hiratsuka, Res. Chem. Intermed. 18 (1992) 131–182;
(g) H. Shizuka, K. Okazaki, M. Tanaka, M. Ishikawa, M. Sumitani, K. Yoshihara, Chem. Phys. Lett. 113 (1985) 89–92.
- [2] H. Sakurai, J. Organomet. Chem. 200 (1980) 261–286.
- [3] (a) G.W. Sluggett, W.J. Leigh, J. Am. Chem. Soc. 114 (1992) 1195–1201;
(b) G.W. Sluggett, W.J. Leigh, Organometallics 11 (1992) 3731–3736;
(c) W.J. Leigh, G.W. Sluggett, J. Am. Chem. Soc. 115 (1993) 7531–7532;
(d) G.W. Sluggett, W.J. Leigh, Organometallics 13 (1994) 1005–1013;
(e) G.W. Sluggett, W.J. Leigh, Organometallics 13 (1994) 269–281.
- [4] (a) O. Brede, R. Hermann, S. Naumov, G.P. Perdikomatis, A.K. Zarkadis, M.G. Siskos, Chem. Phys. Lett. 376 (2003) 370–375;
(b) O. Brede, R. Hermann, S. Naumov, A.K. Zarkadis, G.P. Perdikomatis, M.G. Siskos, Phys. Chem. Chem. Phys. (2004) 2267–2275;
(c) O. Brede, G.R. Mahalaxmi, S. Naumov, W. Naumann, R. Hermann, J. Phys. Chem. A 105 (2001) 3757–3764;
(d) G.R. Mahalaxmi, R. Hermann, S. Naumov, O. Brede, Phys. Chem. Chem. Phys. (2000) 4947–4955.
- [5] M. Kira, H. Yoshida, H. Sakurai, J. Am. Chem. Soc. 107 (1985) 7767–7768.
- [6] (a) H. Hiratsuka, S. Kobayashi, Y. Minegishi, M. Hara, T. Okutsu, S. Murakami, J. Phys. Chem. A. 103 (1999) 9174–9183;
(b) H. Hiratsuka, Y. Kadokura, H. Chida, M. Tanaka, M. Kobayashi, T. Okutsu, M. Oba, K. Nishiyama, J. Chem. Soc. Faraday Trans. 92 (1996) 3035–3041;
(c) We repeated and confirmed the LFP results reported for $\text{Ph}_2\text{CH-SiMe}_3$ by Hiratsuka et al. [6a] and found a quantum yield for the photo-Fries product **DP-CHT** $\Phi \approx 0.95$ and $\Phi \approx 0.05$ for the $\text{Ph}_2\text{CH}^\bullet$ radical. The absorption coefficient ϵ for **DP-CHT** was estimated via the correlation [7a] as $9200\text{M}^{-1}\text{cm}^{-1}$. The increased quantum yield for **DP-CHT** as contrasted to the xanthenyl counterpart **1CHT** ($\Phi = 0.70$) may reflect the predicted by theory [6d,e] and experiment [6f] increased sluggishness of the primary formed radicals to escape the solvent cage as their volume increases, though many other parameters (excitation energy, bond strengths, or other photophysical properties) should play an important role;
(d) R.M. Noyes, J. Am. Chem. Soc. 78 (1956) 5486–5490;
(e) T. Koenig, H. Fisher, in: J.K. Kochi (Ed.), Cage Effects in Free Radicals, vol. 1, Wiley, NY, 1973, p. 157;
(f) E. Schulte, T.J.R. Weakley, D.R. Tyler, J. Am. Chem. Soc. 125 (2003) 10319–10326.
- [7] (a) A.K. Zarkadis, V. Georgakilas, G.P. Perdikomatis, A. Trifonov, G.G. Gurzadyan, S. Skoulika, M.G. Siskos, Photochem. Photobiol. Sci. 4 (2005) 469–480;
(b) G.P. Perdikomatis, Photodissociation vs. photo-Fries rearrangement. The case of benzylsilanes, Ph.D. Thesis, University of Ioannina, Greece, 2004.
- [8] (a) M.B. Ryzhikov, A.N. Rodionov, O.V. Nesterova, D.N. Shigorin, Russ. J. Phys. Chem. 62 (1988) 552–554;
(b) G.G. Huang, D. Huang, P. Wan, J. Org. Chem. 56 (1991) 5437–5442.
- [9] (a) V. Georgakilas, G.P. Perdikomatis, A.S. Triantafyllou, M.G. Siskos, A.K. Zarkadis, Tetrahedron 58 (2002) 2441–2447;
(b) W. Schulten, Ph.D. Thesis, University of Dortmund, Germany, 1977, p. 115.
- [10] (a) J.N. Demas, G.A. Crosby, J. Chem. Phys. 75 (1971) 991, The quantum yield was calculated from the following equation: $\Phi_S = \Phi_F(F_S/F_r) \cdot (A_r/A_s) \cdot (n_r/n_s)$. In the above expression, Φ_S is the fluorescent quantum yield, F the integration of the emission intensities, n the index of refraction of the solution and A is the absorbance of the solution at the exciting wavelength. The subscripts ‘r’ and ‘s’ denote the reference and unknown samples, respectively;
(b) V. Wintgens, L. Jonson, J.C. Scaiano, J. Am. Chem. Soc. 110 (1988) 511–517;
(c) R.V. Bensasson, J.-C. Gramain, J. Chem. Soc. Faraday Trans. 1 76 (1980) 1801–1810.
- [11] S.L. Murov, I. Carmichael, G.L. Hug, Handbook of Photochemistry, second ed., Marcel Dekker, Inc., New York, 1993.
- [12] (a) M.F. Clifton, D.J. Fenick, S.M. Gaspar, D.E. Falvey, M.K. Boyd, J. Org. Chem. 59 (1994) 8023–8029;
(b) T. Sumiyoshi, S. Ueta, F. Wu, S. Sawamura, Radiat. Phys. Chem. 57 (2000) 157–166;
(c) T. Sumiyoshi, S. Ueta, S. Sawamura, Radiat. Phys. Chem. 60 (2001) 331–336;
(d) A. Marcinek, J. Rogowski, J. Adamus, J. Gebicki, M.S. Platz, J. Phys. Chem. 100 (1996) 13539–13543;
(e) F.L. Cozens, M.L. Cano, H. Garcia, N.P. Schepp, J. Am. Chem. Soc. 120 (1998) 5667–5673;
(f) K. Mochida, M. Wasaka, Y. Sakaguchi, H. Hayashi, J. Am. Chem. Soc. 109 (1987) 7942–7947.
- [13] G. Gurzadyan, H. Görner, Chem. Phys. Lett. 319 (2000) 164–172.
- [14] G.G. Gurzadyan, S. Steenken, Chem. Eur. J. 7 (2001) 1808–1815.
- [15] (a) M.J. Frisch, G.W. Trucks, H.B. Schlegel, G.E. Scuseria, M.A. Robb, J.R. Cheeseman, V.G. Zakrzewski, J.A. Montgomery Jr., R.E. Stratmann, J.C. Burant, S. Dapprich, J.M. Millam, A.D. Daniels, K.N. Kudin, M.C. Strain, O. Farkas, J. Tomasi, V. Barone, M. Cossi, R. Cammi, B. Mennucci, C. Pomelli, C. Adamo, S. Clifford, J. Ochterski, G.A. Petersson, P.Y. Ayala, Q. Cui, K. Morokuma, D.K. Malick, A.D. Rabuck, K. Raghavachari, J.B. Foresman, J. Cioslowski, J.V. Ortiz, B.B. Stefanov, G. Liu, A. Liashenko, P. Piskorz, I. Komaromi, R. Gomperts, R.L. Martin, D.J. Fox, T. Keith, M.A. Al-Latham, C.Y. Peng, A. Nanayakkara, M. Challacombe, P.M.W. Gill, B. Johnson, W. Chen, M.W. Wong, J.L. Andres, C. Gonzalez, M. Head-Gordon, E.S. Replogle, J.A. Pople, 1998. GAUSSIAN 98, Revision A.9. Gaussian, Inc., Pittsburgh, PA;
(b) W.J. Hehre, L. Radom, P.v.R. Schleyer, J.A. Pople, Ab Initio Molecular Orbital Theory, Wiley, New York, 1986;
(c) T.H. Dunning Jr., J. Chem. Phys. 90 (1989) 1007–1023;
(d) J.B. Foresman, J.E. Frisch, Exploring Chemistry with Electronic Structure Methods, Gaussian, Inc., Pittsburgh, PA, 1996;
(e) J.B. Foresman, H.B. Schlegel, Application of the Csisingles method in predicting the energy, properties, and reactivity of molecules in their excited states, in: R. Fausto (Ed.), Molecular Spectroscopy: Recent Experimental and Computational Advances, NATO–ASI 77 Series C, Kluwer Academic, The Netherlands, 1993;
(f) J.B. Foresman, M. Head-Gordon, J.A. Pople, M.J. Frisch, J. Phys. Chem. 96 (1992) 135–149;
(g) J. Del Bene, H.H. Jaffe, J. Am. Chem. Soc. 107 (1985) 7767.
- [16] T. Chakraborty, E.C. Lim, J. Chem. Phys. 98 (1993) 836–840.
- [17] (a) T. Schaefer, R. Sebastian, Can. J. Chem. 68 (1990) 1548–1552;
(b) H.S. Kasmai, R. Liu, J. Chem. Soc. Perkin Trans. 2 (1997) 1605–1608.
- [18] (a) J. Nagy, J. Réffy, A. Kuzsman-Borbély, K. Pálóssy-Becker, J. Organomet. Chem. 7 (1967) 393–404;
(b) H. Bock, H. Alt, H. Seidl, J. Am. Chem. Soc. 91 (1969) 355–361;
(c) W. Hasnstein, H.J. Berwin, T.G. Traylor, J. Am. Chem. Soc. 92 (1970) 7476–7477;
(d) G.D. Hartmann, T.G. Traylor, J. Am. Chem. Soc. 97 (1975) 6147–6151;
(e) C.G. Pitt, J. Organomet. Chem. 61 (1973) 49–70;
(f) M.A. Brook, Silicon in Organic, Organometallic, and Polymer Chemistry, Wiley, NY, 2000, pp. 480–510 (Chapter 14);
(g) C. Hansch, A. Leo, R.W. Taft, Chem. Rev. 91 (1991) 165–195.
- [19] S.S.C. Chu, H.T. Yang, Acta Crystallogr. B33 (1977) 2291–2293.
- [20] E. Rochlin, Z. Rappoport, J. Am. Chem. Soc. 114 (1992) 230–241.
- [21] A.C. Blackburn, A.J. Dobson, R.E. Gerkin, Acta Crystallogr. C52 (1996) 1486–1488.
- [22] N.I. Tzerpos, A.K. Zarkadis, R.P. Kreher, L. Repas, M. Lehnig, J. Chem. Soc. Perkin Trans. 2 (1995) 755–761.
- [23] G. Bouchoux, J. Dagaut, Org. Mass Spectrom. 16 (1981) 246–428.
- [24] (a) W. Nakanishi, S. Hayashi, Y. Kusuyama, T. Negoro, S. Masuda, H. Mutoh, J. Org. Chem. 63 (1998) 8373–8379;
(b) C. Ley, F. Morlet-Savary, J.P. Fouassier, P. Jaques, J. Photochem. Photobiol. A: Chem. 137 (2000) 87–92.
- [25] W.A. Pryor, W.D. Graham, J.G. Green, J. Org. Chem. 43 (1978) 526–528.

- [26] S. Lochbrunner, M. Zissler, J. Piel, E. Riedle, A. Spiegel, T. Bach, J. Chem. Phys. 120 (2004) 11634–11639.
- [27] M.A. Miranda, in: W.M. Horspool, P.S. Song (Eds.), CRC Handbook of Organic Photochemistry and Photobiology, CRC Press, Boca Raton, FL, 1994, p. 570;
W. Gu, R.G. Weiss, J. Photochem. Photobiol. C: Photochem. Rev. 2 (2001) 117–137;
J. Xu, R.G. Weiss, Photochem. Photobiol. Sci. 4 (2005) 210–215.
- [28] The Bond Dissociation Enthalpy (BDH) of the C–Si bond in **1** is estimated as 67.5 ± 2.9 kcal/mol, based on the BDH (9,9'-bixanthene) = 35.1 kcal/mol [28a] and $\text{BDH}(\text{Me}_3\text{Si}-\text{SiMe}_3) = 79.3 \pm 2.9$ kcal/mol [28b] and applying Hess-law as suggested by Zavitsas and co-workers [28c];
(a) C. Herberg, H.-D. Beckhaus, C. Rüchardt, Chem. Ber. 127 (1994) 2065–2072;
(b) R. Becerra, R. Walsh, in: Z. Rappoport, Y. Apeloig (Eds.), The Chemistry of Organic Silicon Compounds, vol. 2, Wiley, NY, 1998, p. 153;
(c) N. Matsunaga, D.W. Rogers, A.A. Zavitsas, J. Org. Chem. 68 (2003) 3158–3172.